Endogenous bystander killing mechanisms enhance the activity of novel FAP-CAR-T cells against glioblastoma

Wenbo Yu[1, 2*], Lisa M. Ebert[1, 2, 3*], Nga Truong[1, 2], Ruhi Polara[1], Kevin K. He[1,4], Tessa Gargett[1, 2, 3], Erica Yeo[1, 2], and Michael P. Brown[1,2, 3]

[1] Centre for Cancer Biology, SA Pathology and University of South Australia, Australia

[2] Cancer Clinical Trials Unit, Royal Adelaide Hospital, Adelaide, SA, Australia

[3] School of Medicine, The University of Adelaide, Adelaide, SA, Australia

[4] UniSA Clinical and Health Sciences, University of South Australia, Adelaide, SA, Australia

* The first two authors contributed equally to this study.

Running Title: Bystander killing enhances FAP-CAR-T cells targeting GBM

Key words: CAR-T, glioblastoma, bystander killing, Fibroblast activation protein, glioma neural stem cells.

Additional information:

This work was supported by a Beat Cancer Project Hospital Support Package (MPB), the Neurosurgical Research Foundation (LE, MPB, TG), Tour de Cure (LE, MPB), the Ray & Shirl Norman Cancer Research Trust (LE, MPB), and the Health Services Charitable Gifts Board Adelaide.

Corresponding Author: Lisa Ebert, email lisa.ebert@sa.gov.au

Conflicts of Interest: The authors declare no conflict of interest.

Word count:

Total number of figures: 6

Total number of tables: 1

Abstract

CAR-T cell therapies are being intensely investigated as a novel immunotherapy approach for glioblastoma (GBM), but so far clinical success has been limited. We recently described FAP as an ideal target antigen for GBM immunotherapy, with expression on tumor cells and tumor blood vessels occurring frequently in patients' tumors but with very limited expression in healthy tissues. Here, we generated a novel FAP-targeting CAR with CD3ζ and CD28 signaling domains and tested the resulting CAR-T cells for their ability to lyse GBM cells in vitro and in vivo. FAP-CAR-T cells showed target specificity against model cell lines and exhibited potent cytotoxicity against patient-derived glioma neural stem (GNS) cells. Remarkably, complete destruction of tumor cells was observed even where the antigen was expressed by a minor subpopulation of cells, indicating a bystander killing mechanism. Using co-culture assays, we confirmed the ability of FAP-CAR-T cells to mediate bystander killing of antigen-negative tumor cells, but only after activation by antigen-expressing target cells. This bystander killing effect was at least partially mediated by soluble factors. We also observed that the non-transduced fraction of the CAR-T cell product could be activated via T cell-secreted IL-2 to mediate antigen-non-specific killing, further amplifying the bystander effect. FAP-CAR-T cells controlled without overt toxicity the growth of subcutaneous tumors created using a mixture of antigen-negative and antigen-positive GBM cells. Together, our findings advance FAP as a leading candidate for clinical CAR-T cell therapy of GBM and highlight under-recognized antigen non-specific mechanisms that may contribute meaningfully to the antitumor activity of CAR-T cells.

Introduction

Glioblastoma multiforme (GBM) is the most lethal form of primary brain tumor and there is an urgent need for more effective therapies. Despite receiving intensive treatment upon initial diagnosis with all three classical pillars of cancer therapy (surgery, radiotherapy, and chemotherapy), patients almost inevitably relapse within a matter of months. There is no standard treatment for recurrent GBM, and most patients will die within 6 months of recurrence(1). The recent emergence of a 'fourth pillar' of cancer treatment, immunotherapy, may provide new hope that this dismal picture can be changed.

Chimeric antigen receptor (CAR)-T cells are one of the success stories of cancer immunotherapy, but so far clinical impacts are limited to B-cell malignancies. There remain significant hurdles to overcome before this success can be extended to solid tumors(2). One clear challenge is the lack of ideal target antigens in solid tumors, in contrast to B-cell malignancies where lineage markers, such as CD19, show near-ubiquitous expression on cancerous cells and no expression outside the hematologic compartment. Nevertheless, the possibility of adapting CAR-T cell therapy to the treatment of GBM is under extensive investigation(3). Most interest to date for clinical CAR-T targeting of GBM has focused on targeting the antigens EGFRvIII, HER2 and IL-13R2α(4-9). And although encouraging studies are in progress, positive outcomes from clinical trials to date have been modest, with only a single patient reported to undergo complete albeit non-durable tumor regression in response to a CAR-T cell treatment(6). Given the profound tumor heterogeneity of GBM, identification of more and better targets is a key focus of research.

Fibroblast activation protein (FAP) is a surface-expressed proteolytic enzyme that is well known for its expression in cancer-associated fibroblasts(10). Because of this, FAP has been identified as a promising immunotherapy target for carcinomas which are typically heavily infiltrated with fibroblasts, such as those of prostate, breast, lung, and pancreas. In those studies, FAP has primarily been investigated as the target of tumor supporting stroma(11-14), but can also serve as a direct tumor target in certain cancers such as mesothelioma(15,16). We and others found FAP to be consistently over-expressed in GBM compared to normal brain, although we failed to find fibroblast expression of FAP in GBM(17,18). Rather, our detailed expression analyses of all cell types in GBM revealed heterogeneous expression of FAP on the tumor cells, coupled with near-ubiquitous expression around tumor blood vessels, with expression observed on both endothelial cells and pericytes. These studies suggest FAP is an ideal immunotherapy target for GBM, as it should allow targeting of not only tumor cells, but also the tumor's supporting vascular networks(17).

FAP-specific CARs have been described in the literature. All FAP-CARs have been derived from one of four mouse monoclonal antibodies (mAbs). A CAR developed from the FAP-5 mAb cross-reacts with both mouse and human FAP. However, FAP-5-CAR-T cells showed serious toxicities in mice and this CAR has not been pursued further(19). A second CAR developed from the F19 mAb recognizes only human FAP, thus this CAR could not be used to test potential host FAP-related toxicities in mouse models (15,16,20). A third CAR developed from mAb 73.3 cross-reacts with both mouse and human FAP and showed limited toxicities in mice(13,14). CAR-T cells derived from both F19 and 73.3 mAbs showed antitumor effects in mouse models of multiple types of transplanted tumors(13,16) and have now progressed into phase 1 clinical trials (ClinicalTrials.gov Identifiers: NCT039325652019 and

NCT017221492015). However, neither CAR-T has been tested on GBM. F19-CAR-T cells were well tolerated clinically(21), although no detailed report of either trial has been released yet.

In this study, we generated a FAP-specific CAR derived from the MO36 mAb, which was selected from phage display and recognizes both murine and human FAP(22). Another CAR based on MO36 previously showed antitumor effects in a lung cancer mouse model without toxicity(12). We tested FAP-CAR-T cell function using model cell lines, tumor cells expanded from patient GBM tissues, and a mouse model designed to recapitulate the natural heterogeneity of GBM. In addition to confirming the specificity and activity of FAP-CAR-T cells, we also uncovered a potent bystander killing mechanism that could facilitate more complete tumor destruction than would be predicted by antigen expression alone.

Materials and methods

Tumor cell lines

All cell lines and GNS cells used in this study are listed in Table S1. U251, U87 and RPMI-7951 cell lines were obtained from ATCC. U251-GFP and U87-RFP were a kind gift from Professor Stuart Pitson (Centre for Cancer Biology, Adelaide). All cells were maintained in Minimum Essential Medium Eagle supplemented with 10% fetal bovine serum (FBS), 1% penicillin/streptomycin, 1% glutamax, 1% sodium pyruvate, and 1% MEM non-essential amino acid solution (all ThermoFisher Scientific). Short-term cultured GNS cell lines were a kind gift from Professor Bryan Day (QIMR Berghofer Medical Research Institute, Brisbane) or were generated in our laboratory as described(17,23). GNS cell lines were cultured in StemPro Neural Stem Cell medium (StemPro NSC, ThermoFisher Scientific) in flasks, which were pre-coated with Matrigel (Corning) diluted 1/100 in PBS according to the manufacturer's recommendations. Cultures were passaged using Accutase (ThermoFisher) when they reached ~70-90% confluence.

CAR transgene design and construction

Anti FAP scfv with Myc tag was obtained by PCR using donated plasmid containing MO36 as a template. The primers were F: GCCCGACGTCGCCACCatggactggatctggcgcatc ; R: TGCGGCCCCATTCAGATCCTCTTCTGAGATGAGTTTTTGTTCTGCGGCCGCCCGTTTTATTTCCAGC. A human IgG4 hinge/CH2CH3 was chosen as a long spacer to reduce the affinity to human FcRs(24,25). Aiming to avoid activation-induced cell death by further reducing its affinity to human and murine FcRs, additional modifications were made to the CH2 region. Three amino acid (PVA) derived from IgG2 substituted for four amino acids (EFLG) in the corresponding

126 region of IgG4, and another glycosylation motif was mutated from N to Q(26,27). The CD3ζ
127 and CD28 signaling domains were positioned after the spacer. Hinge, spacer and signaling
128 domains were synthesized by GeneArt. All fragments were assembled on pEntry vector and
129 subcloned into lenti vector pPHLV-A.

130 ***Generation of CAR-T cells***

131 HEK293T cells in a T175 flask were transfected with 46.4µg DNA consisting of equal amounts
132 of four plasmids using 138µL lipofectamine 2000 (ThermoFisher). The plasmids were: (i)
133 pHLVA-FAP-CAR, which provides the lentiviral RNA containing the CAR; (ii) pMD2.G, which
134 provides expression of VSV-G; (iii) pMDLgpRRE, which provides expression of gag pol; and (iv)
135 pRSV-REV which provides the rev gene for lentiviral packaging. The supernatant was
136 harvested 48h after transfection, centrifuged at 500 x *g* for 10min. and filtered through a
137 0.45µm filter (Nalgene™ Rapid-Flow™), ready for transduction. To produce CAR-T cells, a 24-
138 well plate was pre-coated with anti-CD3 (OKT3) and anti-CD28 antibodies (15E8) (Miltenyi
139 Biotec) at 1µg/mL on day 0. PBMC were seeded at 1×10^6 cells/well on day 1 in Advanced
140 RPMI (ThermoFisher) with 10% FBS, with IL-7 and IL-15 (Miltenyi Biotec) added at 10ng/mL
141 and 5ng/mL, respectively, on day 2. On day 3, the activated T cells were transduced by
142 spinoculation with lentivirus encoding FAP-CAR. In brief, 0.5mL T cells at 2×10^6 cells/mL were
143 mixed with 1.5mL lentiviral supernatant and centrifuged in 24-well plates pre-coated with
144 7µg/mL Retronectin (Takarabio) at 1000 x *g* for 20min. The transduced T cells were expanded
145 for another 4 days with IL-7/IL-15 before being cryopreserved in FBS + 10% DMSO and stored
146 in liquid nitrogen. Before use, the CAR-T cells were thawed and rested overnight in Advanced
147 RPMI with 10% FBS. CAR expression was detected by FITC-conjugated anti-myc tag antibody

(Abcam) and analyzed by flow cytometry using an Accuri C6 Plus flow cytometer (BD Bioscience, Franklin Lakes, NJ, USA).

IL-2 assay

Target cells were seeded in a flat-bottom 96-well plate at 20,000 cells/well on day 0. On day 1, the plate was topped up with 1×10^5 CAR-T cells per well. The supernatant was collected on day 3 and analyzed by human IL-2 ELISA Kit (ThermoFisher) according to the manufacturer's protocol.

Flow cytometry analysis of FAP expression

U251, U87 and RPMI-7951 cells were stained by PE-conjugated anti-FAP antibody (clone 427819, R&D Systems) in 5% BSA/PBS staining buffer for 30min. Cells were washed with staining buffer and 1µL 7AAD (ThermoFisher) was added in a final resuspension volume of 200µL before analysis by flow cytometry (BD Accuri™). For staining of GNS cultures, cells were harvested using Accutase (ThermoFisher), washed in PBS and resuspended in FACS buffer (PBS + 1% bovine serum albumin + 0.04% sodium azide). Cells were then stained as described above.

Cytotoxicity assay using real-time impedance-based cell analysis

The Axion BioSystems Maestro Z system was used to measure cytotoxicity. After addition of 100µL of culture medium to the plate, a baseline reading was taken and then target cells were seeded in a volume of 100µL at 15,000 cells/well for U87 and U251 or 10,000 cells/well for GNS cultures. The wells were pre-coated with Matrigel if GNS cells were used as targets. Resistance values were monitored every 60sec using AxisZ software during overnight culture

at 37℃ in the Maestro Z instrument. Once formation of a stable monolayer was confirmed, 100µL of CAR-T cells were added in the same medium as the target cells. Resistance values were normalized to a time shortly after adding CAR-T cells once readings had re-stabilized. Cytotoxicity was measured as %lysis based on the impedance ratio of tested cells and untreated control cells, which was calculated by AxisZ software.

Cytotoxicity assay by flow cytometry

GNS cells (1 x 10^5) were co-cultured with an equal number of FAP-CAR-T cells or control non-transduced T cells (NT-T) in equivalent culture conditions in StemPro NSC medium in a 24-well plate. In co-cultures of pairs of GNS cell lines of differing levels of FAP expression, FAP-expressing GNS cells were first pre-labeled with CellTrace™ Far Red (CTFR; ThermoFisher) at 1µM for 20min at 37^0C, to differentiate the populations, and equal numbers of FAP(+) and FAP(-) cells were mixed. Cells were harvested after 48h co-culture with T cells and stained in PBS with Fixable Viability Stain 575V (BD) or Fixable Viability Dye eFluor™ 506 (Invitrogen) where indicated for 10min at room temperature, before antibody staining. The antibodies used for staining included: BB515 anti-Fas (clone DX2, BD Biosciences), BV786 anti-CD3 (clone SK7, BD Biosciences), PE anti-FAP (clone 427819, R&D Systems) and BV480 anti-FasL (clone NOK-1, BD Biosciences). Samples were acquired on an LSR Fortessa (BD Biosciences) and data analyzed using FCS Express 7 Cytometry (De Novo software, Pasadena, CA, USA).

Cytotoxicity assay to assess the role of soluble factors

These experiments were conducted in 24-well Transwell plates (Corning) or Nunc Cell Culture Inserts (ThermoFisher) with a 0.4µm pore size. FAP-expressing cells were plated in the lower well at 1 x 10^5 cells/well, and 1 x 10^4 FAP-negative cells were seeded in the upper inserts.

When monolayers of target cells had established, FAP-CAR-T cells or non-transduced T cells were added to the bottom well at a 1:1 E:T ratio. After 48h incubation at 37°C, cells in the inserts were stained using propidium iodide (PI) (ThermoFisher) at 1µg/mL and Hoechst 33342 (ThermoFisher) at 2µM for 20min at 37°C. Without washing, inserts were imaged using an IX73 microscope equipped with CoolLED pE-4000 light source and running CellSens software (Olympus). The cells on each image were counted by QuPath (University of Edinburgh). Cell viability was calculated as [1 - (PI counts/Hoechst counts)] x 100%.

Cytotoxicity assay using fluorescence imaging of U87-RFP and U251-GFP cells

U87-RFP and U251-GFP were seeded with starting numbers of 5×10^4 cells/well. FAP-CAR-T cells were immediately added at a 1:1 E:T ratio. The cocultured cells were imaged by the Olympus IX73 microscope 24h later using 100ms exposure for RFP and 3ms exposure for GFP. Three fields of views were taken from each well and duplicate wells were used for one assay. The images were analyzed by ImageJ for fluorescence counts using threshold values of 68-255 for RFP and 98-255 for GFP. All images were collected and analyzed using the same parameters for consistency.

Measurement of secreted cytotoxic factors

Supernatants were collected from the cytotoxicity assays conducted in the Maestro Z instrument at the end point time and stored at -20°C until use. Levels of soluble factors were quantified simultaneously using the LEGENDplex Human CD8/NK Panel (BioLegend), according to the manufacturer's protocol. Samples were analyzed using a BD LSR Fortessa.

Murine subcutaneous tumor xenograft model

Animal experiments were approved by the University of South Australia Animal Ethics Committee (Ethics number: 45/17). Nonobese diabetic/severe combined immunodeficiency/IL2Rgamma-null (NSG) mice were purchased at 6 weeks from the Animal Resource Centre (Perth). To create tumors of mixed cell populations, an admixture of 1×10^6 U251-GFP cells and 2×10^6 U87-RFP cells were injected subcutaneously in both flanks. Tumors were allowed to establish for 11 days and then 1×10^6 CAR-T cells were administered by tail vein injection. Mice were monitored daily until tumors became palpable, after which time tumor growth was measured using an electronic caliper every 2-3 days. The volume of the tumor was calculated as length × width^2 ×1/2. Mice were humanely killed when at least one tumor volume reached 1000mm^3. Tumors were harvested at the experimental end point and prepared for frozen sections. Tumor samples fixed in 10% buffered formalin overnight were cryoprotected with 10% sucrose to 30% sucrose in PBS sequentially before embedding in OCT (Sakura) and freezing on dry ice, with subsequent storage at -80^{o}C. This protocol was selected and optimized to allow maximum retention of soluble fluorescent proteins (GFP/RFP) during tissue processing. Cryosections (5µM) were cut using a Leica CM1950 cryostat and mounted using ProLong Gold with DAPI (ThermoFisher). Slides were imaged using the Olympus IX73 microscope. Tumour tissue was located microscopically by DAPI staining. To minimize bias, photographs were taken for the GFP or RFP channels and areas of green and red fluorescence, respectively, were automatically calculated using ImageJ (NIH). Threshold 21-255 was used for RFP area calculation while threshold 35-255 was used for GFP area calculation. Fluorescence overlays were created by overlaying black and white images and applying false colors using ImageJ.

235 ***Statistical analysis***

236 Statistical analyses were performed using GraphPad Prism version 5 and OriginPro 8
237 (OriginLab). In addition, the TumGrowth web program
238 (https://kroemerlab.shinyapps.io/TumGrowth/) (cite PMID: 30228932) was used for
239 comparison of tumor growth curves by Type II ANOVA. For Kaplan-Meier Survival analysis, Log
240 Rank method was used to test the Equality over Groups.

241

Results

Generation and production of CAR T cells targeting FAP

Based on previous studies(12,22), we designed and constructed a FAP-CAR comprising the MO36 single chain fragment-variable (scFv), a myc epitope tag, a long spacer, and CD28 and CD3ζ signaling domains (Figure 1A). This CAR transgene was integrated in CD3/CD28-activated human T cells via lentiviral transduction. CAR expression on transduced T cells was assessed by flow cytometry (Figure 1B). Transduction efficiency values sufficient to test CAR-T cell function (~15-25%) were achieved using unconcentrated viral supernatant.

CAR-T cell responses to FAP stimulation in vitro were initially measured by co-culturing CAR-T cells with FAP-expressing long-term cancer cell lines. The RPMI-7951 melanoma cell line, which expresses uniformly high levels of FAP, was used as a FAP-CAR-T (FAP-T) cell quality control. RPMI-7951 cells were co-cultured with FAP-T cells for 48 hours, and the level of IL-2 in the culture supernatant was measured by ELISA (Figure 1C). The FAP-negative U251 GBM cell line was used as a negative control. The data indicate that FAP-T cells responded specifically to target cells expressing FAP.

Cytotoxicity of FAP-CAR-T cells against GBM cell lines and patient-derived glioma neural stem (GNS) cells

We next used impedance-based real-time analysis to assess FAP-T cell cytotoxicity. The FAP-expressing U87 human GBM cell line was used as the target in this assay (Figure 2A) and compared with the FAP-negative GBM cell line U251. As expected, FAP-T cells were strongly

cytotoxic against U87 target cells, whereas non-transduced T cells (NT-T) induced only minimal background lysis. FAP -T cells failed to lyse U251 cells above background levels, thereby confirming the specificity of the CAR.

Although long-term established cell lines such as U87 provide a suitable model to test a diverse range of therapeutic approaches, these cells may not adequately represent primary GBM cells. Therefore, we next selected a panel of patient-derived glioma neural stem (GNS) cells as a more biologically relevant type of target cell to test the cytotoxic activity of our FAP-T cells. We checked a panel of different GNS cells for FAP expression and chose three cultures which express different levels of FAP. CCB-G3-C, MN1, and CCB-G6-T are representative of high, medium, and low level FAP expression, respectively (Figure 2B). We found substantial killing of all of three GNS cell lines (Figure 2B). Of note, when cultured with MN1 cells, which are <50% FAP(+), the FAP-T cells induced near-complete cytotoxicity (> 90% lysis). Even more remarkably, in the case of CCB-G6-T cells, even a 10% FAP(+) population was sufficient to induce the lysis of >80% of all target cells.

Hence, our observations in the real-time cytotoxicity assay suggested a potential bystander killing mechanism in this system (28). We therefore used flow cytometry to further investigate the effect of FAP-T cells on FAP(+) and FAP(-) subpopulations of the CCB-G6-T cell line. CCB-G6-T target cells were co-cultured with FAP-T cells for 48 hours. After this time, the small FAP(+) population within CCB-G6-T was depleted from 6.5% to 1.5%, as expected. Notably, however, the total loss in cell viability was ~70%, far more than the FAP(+) population, further suggesting a bystander killing effect of FAP-T cells (Figure S1).

Confirmation that FAP-CAR-T cells induce antigen-dependent bystander killing of tumor cells

One question is whether the bystander killing was mediated by low-level expression of FAP, which was not detected by flow cytometry but was still sufficient to trigger CAR-T killing. If bystander cytotoxicity is genuine, then killing of antigen-negative target cells should be observed only after the CAR-T cells are activated by antigen-positive target cells. To test this, we labeled FAP(+) GNS cell lines with a fluorescent dye (CellTrace Far Red; CTFR) and mixed them with unlabeled GNS cells lacking FAP expression. This target-cell mixture was incubated with FAP-T cells or NT-T cells for 48 hours and the viability of each target-cell population was analyzed by flow cytometry (Figure 3A). Two different pairs of FAP(+)/FAP(-) GNS cell lines were used- Pair 1: FAP(+) MN1 with FAP(-) RKI1, and pair 2: FAP(+) CCB-G3-C with FAP(-) SJH1. Whereas MN1 and CCB-G3-C cells showed uniform expression of FAP by flow cytometry, RKI1 and SJH1 cells lacked any detectable surface expression (Figure 3B). These FAP-negative GNS cells also lacked significant gene expression by microarray analysis (data not shown).

As expected, the viability of FAP-negative tumor cells cultured alone was not affected by incubation with FAP-T cells, thereby ruling out off-target effects. But when FAP(-) target cells were mixed with FAP(+) target cells and subsequently incubated with FAP-T cells, significant killing of the FAP(-) tumor cells was observed (Figure 3C-D). Thus, FAP-T cells can exert substantial bystander killing of tumor cells lacking FAP, but only once they have been activated by cells expressing their cognate antigen. To determine if the bystander killing effect is unique to FAP-T cells, we also tested GD2-specific CAR-T cells on GNS cells expressing low levels of GD2 (16-26% GD2+). Real-time cytotoxicity assays revealed complete lysis of these

target cells despite heterogeneous antigen expression (Figure S2), thus suggesting that the bystander killing activity of CAR-T cells is not restricted to a particular CAR.

Bystander cytotoxicity occurs independently of Fas/FasL but can be mediated by soluble factors

Bystander killing of antigen-negative targets has recently been reported to occur via Fas-FasL interactions(28). To determine if this molecular axis was at play in our system, we first investigated expression of Fas on our GNS cell lines, and expression of FasL on our FAP-T cells. Although variable levels of Fas were detected on the GNS cell lines (RKI1, SJH1 and CCB-G6-T) found to be susceptible to bystander killing (Figure S3A), there was almost no expression of FasL by FAP-T cells, even after co-culture with FAP(+) target cells and with permeabilization to detect intracellular stores of FasL (Figure S3B). Soluble FasL in culture medium was also low (< 20pg/mL, data not shown). ZB4 was reported as a function-blocking anti-Fas antibody(29). We confirmed this in our soluble FasL induced cytotoxicity assay (Figure S3C). However, ZB4 failed to attenuate either direct killing (data not shown) or bystander killing (Figure S3 D-E). We therefore conclude that bystander killing is unlikely to be mediated by Fas/FasL interactions in our system.

We next hypothesized that soluble factors such as cytokines could contribute to the bystander killing effect. This was tested by separating antigen-negative target cells from CAR-T cells using a semi-permeable membrane. FAP-T or NT-T cells were seeded together with FAP(+) GNS cells in the lower chambers of Transwell assemblies, while FAP(-) GNS cells were seeded

in the upper chambers (Figure 4A). After 48 hours, cells in the upper chambers were stained using propidium iodide (PI) to label dead cells and Hoechst 33342 to visualize total nuclei, and cell viability calculated by the ratio of PI/Hoechst-stained cells. The same combinations of FAP(-) SJH-1/FAP(+) CCB-G3C cells and FAP(-) RKI-1/FAP(+) MN-1 cells from Figure 3 were used in this assay. In keeping with our hypothesis, significant killing of FAP(-) tumor cells in the upper chamber (SJH-1 or RKI-1) was observed when FAP-T cells were present in the lower chamber together with FAP(+) tumor cells (Figure 4B-D).

Since the Transwell experiments suggested that bystander killing of antigen-negative cells can be at least partly mediated by soluble factors, a panel of cytokines and cytotoxic proteins was measured in co-culture supernatants. Large amounts of TNF-α, IFN-γ, granzyme A, granzyme B and granulysin were released when FAP-T cells were co-cultured with FAP(+) GNS cells, but not when cultured alone (Figure 4E). Perforin was also detected in the co-culture supernatants but was similarly secreted in the absence of target cells, suggesting constitutive secretion by FAP-T cells. None of these factors was secreted by NT-T cells, even in the presence of FAP(+) GNS tumor cells. Together, our results indicate that FAP-T cells can be activated by antigen to secrete a range of cytotoxic cytokines and proteins, which may contribute to the contact-independent bystander killing observed in the Transwell system.

FAP-CAR-T cell activation mobilizes the CAR-negative T-cell fraction to enhance cytotoxicity

It has long been recognized that, in addition to antigen-dependent cytotoxicity, T cells can also undergo cytokine-induced bystander activation (30). Our FAP-T cell products contain

~75% CAR-negative T cells, leading us to hypothesize that CAR-T cells may secrete cytokines to mobilize the non-transduced T cells into the antitumor response after activation by FAP-expressing tumor cells (Figure 5A). In this way, the whole population of T cells could be synchronized to exert cytotoxicity against both antigen-positive and antigen-negative tumor cells. Cytokines including IL-2, IL-12, IL-15 and IL-21 have been reported to initiate antigen nonspecific T-cell activation(31-33). And although IL-15 and IL-12 are primarily produced by antigen presenting cells, IL-2 and IL-21 can be produced by T cells. We showed that IL-2 was secreted by FAP-T cells after antigen activation (Figure 1D), suggesting that it could be one of the cytokines to mobilize normal T cells during bystander killing.

We performed additional real-time cytotoxicity assays to explore these concepts further by recapitulating the bystander activation and killing processes in vitro. The cytotoxicity of FAP-T cells or NT-T cells was tested against MN1 GNS cells expressing moderate levels of FAP, with or without the addition of exogenous IL-2 (Figure 5B). FAP-T cells displayed strong cytotoxicity against MN1 as expected, which was further boosted by the addition of IL-2. This effect was marginal at high E:T ratios but became more pronounced at lower E:T ratios as CAR-expressing effector cells became limiting. Of note, IL-2 also dramatically increased the cytotoxicity of control T cells. For example, at a high (5:1) E:T ratio, NT-T cells supplemented with IL-2 induced as much tumor cell killing as FAP-T cells.

We further analyzed cytokines and cytotoxic proteins in supernatant samples collected from these assays. In addition to IL-2, we measured another 12 analytes (Figure 5C, Figures S4, Table 1). The addition of IL-2 to NT-T cells significantly increased the levels of all factors except IL-10 and IL-17a (see column 3 in Table 1), suggesting that these two cytokines were

upregulated only by CAR stimulation, not IL-2. Furthermore, by comparing NT-T cells + IL-2 to CAR-T cells + IL-2, we could show that all factors were further boosted by CAR engagement except for perforin (see column 4 in Table 1), suggesting that IL-2 alone was sufficient to induce maximum secretion of soluble perforin. Interestingly, all analytes showed a positive correlation with the extent of cytotoxicity except soluble Fas and FasL (Table 1, column 2). These results agree with those from our ZB4 blocking experiment (Figure S3), which did not support a significant role for the Fas/FasL axis in cytotoxicity in our system.

Besides the soluble cytokines, classic innate-like effector molecules such as NKG2D could also contribute to bystander killing(34). We assessed expression of NKG2D on T cells in the coculture assay (FAP-T/ NT-T with GNS MN1) and found upregulated NKG2D on CD8(+) T cells, both on CAR (+) and CAR (-) populations, but not on the NT-T cells unless IL-2 was added, which provides further evidence to support our bystander killing model (Figure S5).

In summary, our findings suggest that cytokines, such as IL-2 used here, can stimulate the non-transduced fraction of a CAR-T cell product also to mediate tumor cell killing. Furthermore, this amplification of the response may be an important aspect of the bystander killing mechanism, because IL-2 also upregulated the secretion of factors such as TNFα, IFNγ, granzyme and granulysin, which are candidate mediators of bystander killing. Other cytokines upregulated in this system (IL-4, IL-6, IL-10, and IL-17) are not directly involved in cytotoxicity but can support T- and B-cell function.

FAP- T cells control the growth of tumors and increase survival time in a subcutaneous GBM xenograft model despite heterogeneous antigen expression.

To assess the function of our CAR-T cells in vivo, we tested their ability to control the growth of subcutaneous human xenograft tumors in immunodeficient (NSG) mice. GBM tumors are well-known for their cellular heterogeneity, and we have shown that expression of FAP by GBM tumor cells is also heterogenous(17). Accordingly, we generated a model with mixed FAP(+) and FAP(-) cells. FAP(+) U87 cells were engineered to express RFP, while FAP(-) U251 cells were engineered to express GFP, to allow monitoring of the mixed tumor cell populations. In an initial in vitro assay, the single target cell populations or the target cell mixture were co-cultured with FAP-T cells or NT-T cells and surviving cells were counted using fluorescence microscopy 24 hours later. Counts of FAP(-) U251 cells were reduced significantly only in co-cultures of U87 cells and FAP-T cells, suggesting that antigen-negative tumor cells U251 are also susceptible to bystander killing from FAP-T cells (Figure 6A), like our earlier observations using GNS cells.

The fluorescently tagged U87 and U251 cell lines were mixed at a 2:1 ratio, respectively, before subcutaneous implantation in each flank of NSG mice. The 2:1 mixing ratio was selected after an initial pilot study and resulted in the most evenly balanced tumors at endpoint (Figure 6B, S6 A-B). Compared to either NT-T cells or no treatment, intravenous administration of a low dose (1×10^6) of FAP-T cells significantly reduced tumor growth (adjusted $p < 0.0001$ by Type II ANOVA for both control comparisons; Figure 6C), and significantly increased survival time of treated mice (both $p < 0.0001$ by Log-Rank test; Figure 6D). In mice treated with FAP-T cells, both the GFP and RFP signals in necropsied tumor

412 tissues were significantly reduced compared to tumors in either control group (Figure 6E),
413 suggesting CAR-T cell targeting of both FAP(+) U87-RFP and FAP(-) U251-GFP cells. These
414 findings support the effectiveness of our FAP-T cells in controlling the growth of GBM cells in
415 vivo, even in the face of heterogeneous expression of target antigen.

416

Discussion

For many years, FAP has been recognized and tested as a promising immunotherapy target for carcinomas and mesothelioma(11-16). More recently, we have proposed FAP as a candidate immunotherapy target antigen for GBM(17). Studies from our group and others have shown that, in GBM, FAP is heterogeneously expressed on tumor cells themselves, and more consistently by tumor-supporting stromal populations including endothelial cells (ECs) and pericytes. This sits in sharp contrast to the limited expression in healthy tissues and vessels(17,35). Despite all these characteristics, FAP has never been tested as a target antigen for immunotherapeutic strategies in GBM.

GBM has striking tumor heterogeneity(36). Moreover, GBM tumors, like many other cancers, are proposed to have a hierarchical organization originating from cancer stem-like cell proliferation and differentiation(37,38). For initial confirmation of targeting specificity, we used long-term cell lines including U87 and U251, and these studies successfully demonstrated that our FAP-CAR-T cells secrete IL-2 and induce cytolysis only when FAP is expressed. However, these cell lines (which have been cultured for many decades in vitro in the presence of xenogeneic serum) may lose multipotency, develop pro-survival mechanisms and fail to model the disease properly(39). For further in vitro testing, we therefore moved to the use of glioma neural stem (GNS) cell lines, which are patient GBM tissue-derived cells expanded under serum-free conditions to a limited passage number (generally < 30) and maintain a more in vivo-like phenotype(17,38). Our group has developed a panel of GNS cells from patient samples and characterized them for FAP expression(17) and we used these GNS

cells, together with those from the Q-Cell resource(40) as in vitro models to investigate more authentically how our CAR-T cells tackle the heterogeneity of GBM.

Our results using GNS cells in a sensitive real-time cytotoxicity assay indicated that the percentage of cells lysed by FAP-CAR-T cells can greatly exceed the percentage of target cells expressing the antigen. Further flow cytometry-based analysis of co-cultured GNS cells confirmed that FAP-CAR-T cells can kill antigen-negative tumor cells, but only in the presence of antigen-positive tumor cells. These CAR-T cells are therefore capable of 'bystander' killing, a phenomenon long recognized in T-cell immunology but less well understood(41,42). The significance of bystander killing in CAR-T cell function is also just beginning to be appreciated(28,43), and many questions remain. For example, it is unclear whether all CAR-T cell products have bystander killing capacity, or does this depend on factors such as CAR structure or target cell susceptibility? Based on our observation (Fig. 3, S2), we believe that this function may be a general feature of CAR-T mediated toxicity and has been generally underappreciated in the field because it will not have been revealed in such short-term cytotoxicity assays as the classical chromium release assay. By using the novel Maestro Z instrument to track target cell destruction over several days, we allow CAR-T cells the time required to be activated by CAR engagement with antigen-positive tumor cells and then deploy a range of cytotoxic mechanisms against antigen-negative tumor cells. Therefore, it is possible that all CAR-T cell populations can perform bystander killing, but an assay with a long enough observation period is required to record this phenomenon.

Another important question regarding bystander killing is: what are the key effector molecules that drive this process? The major killing mechanism described for CAR-T cells has

been direct cytolysis, which is induced by perforin and granzyme and which is delivered via a CAR-mediated immunologic synapse(44). Recent studies have suggested that the Fas/FasL signaling axis participates in CAR-T cell cytotoxicity, and in bystander killing (28,43). In contrast, we did not find evidence that Fas/FasL contributes to bystander killing (or cytotoxicity in general) by FAP-CAR- T cells. We did, however, observe that the bystander killing effect was at least partly mediated by soluble factors, as significant cytotoxicity was observed even when the CAR-T cells and tumor cells were not in direct contact. Determining exactly which secreted factor or factors drive bystander killing by FAP-T cells is beyond the scope of the present study. However, we did detect secretion of a range of cytokines and cytotoxic granule components upon antigen engagement of FAP-T cells. Two cytokines of particular interest are TNFα and IFNγ, both of which have a direct antitumor effect(45,46). Moreover, TNF has previously been shown to play a critical role in CAR-T cell antitumor activity(47). We also detected secretion of surprisingly high levels of molecules such as granzyme B and perforin, which are normally involved in cytotoxicity mediated by immunologic synapse formation. Whether these molecules mediate cytotoxicity when secreted into the surrounding environment is unclear. Recombinant granzyme B has been reported to mediate apoptosis through Hsp70 internalization(48) and further study is warranted to determine whether natural granzyme B can mediate cytotoxicity through the Hsp70 pathway in our system. Granzyme A has far weaker apoptotic activity than Granzyme B(49). The role of perforin in antigen nonspecific killing is unclear, with contradictory results reported(32,50,51). It is unlikely for freely diffusing perforin to mediate cytotoxicity here because direct contact is probably essential. Granulysin is an antimicrobial peptide, but recent evidence suggests it has antitumor effects(52). One potential mechanism is mediated by

extracellular vesicles(53) and, hence, we cannot rule out a role for granulysin in the bystander killing effect. Also, it should be noted that multiple proinflammatory cytokines can exert synergistic cytotoxicity(54).

Other than direct cytotoxicity by CAR-T cells, we postulate that the non-transduced fraction of a CAR-T cell product significantly contributes to killing of both antigen-positive and antigen-negative tumor cells. Bystander activation of T cells has been observed during viral or bacterial infection and involves activation of T cells in a T-cell receptor-independent and cytokine-dependent manner. IL-18 and IL-15 are important factors that induce bystander activation of T cells(55). In tumor immunology, antigen nonspecific T-cell activation plays an important role in tumor control(30). IL-2 and IL-15 can convert T cells to lymphokine-activated killer (LAK) cells and exert cytotoxicity through antigen-independent mechanisms(32,33).

Of particular interest is IL-2, which was the first chemokine approved for human cancer therapy(56). IL-2 is a master cytokine, which shapes the proliferation, differentiation and function of T cells and which can regulate the cytolytic machinery of T cells, including upregulation of perforin, Granzyme A/B and other proteins required for cytolytic granule fusion(57). In this study, we hypothesize that when stimulated by antigen, CAR-T cells can produce cytokines such as IL-2, which will induce the non-transduced T cells to exert cytotoxicity via antigen-independent mechanisms. We recapitulated this effect through an in vitro cytotoxicity assay, in which the cytotoxicity of normal T cells was promoted with IL-2 (Fig. 5). This IL-2-dependent function may serve to further broaden the antitumor effect of CAR-T products. Besides soluble cytokines, classic innate-like effector molecules such as NKG2D may also contribute to bystander killing(32,34) (Fig. S5). Accordingly, the observed bystander

activation and bystander cytotoxicity may represent a mechanism that bridges innate and adaptive antitumor immunity.

To mimic the heterogeneity of GBM in vivo, we developed a mixed tumor model in which fluorescently tagged U87 and U251 cells were combined in an optimized ratio to produce tumors that had both cell types still present at endpoint. Using this model, we have shown that FAP-CAR-T cells, administered in a single intravenous dose, can significantly delay tumor growth despite antigen heterogeneity. Analysis of tumor tissues at endpoint revealed that both U87 FAP(+) and U251 FAP(-) cells were reduced following FAP-T cell treatment, suggesting that the CAR-T cells exert longitudinal control over both U251 and U87 cells. In these tumors, there were large areas of non-fluorescent tissue, which may come from two sources: nonfluorescent tumor cells that finally escape immune control or infiltrating mouse-derived stromal tissue(58).

Our observations suggest that bystander killing mechanisms may enable CAR-T cells to target more tumor cells than would be predicted from the target antigen expression pattern, and thus may contribute to tumor destruction even in the presence of tumor heterogeneity. Similar or more potent bystander killing effects may be observed by arming CAR-T cells with cytokines such as IL-15(59,60) or IL-2(61), which may be safer than systematically administered cytokine therapy. It was estimated, for example, that under physiologic conditions in dense tissues such as lymph nodes, the cytokine IL-2, interacts over a characteristic length scale of 8-14 cell diameters (80-140 μm), which is determined by a balance between diffusion and consumption of cytokine(62). Therefore, we might expect that

bystander killing effects, which are mediated by soluble factors, may be limited to the tumor microenvironment where CAR-T cells engage with antigen.

In this study, we have developed a novel FAP-targeting CAR and shown, for the first time, that FAP-T cells effectively destroy GBM cells in vitro and in vivo. In addition, we highlight two mechanisms that broaden the anti-tumor effect of our CAR-T cell product: bystander killing of antigen-negative tumor cells, and cytokine-mediated bystander T-cell activation. Future work to better understand these mechanisms may reveal opportunities to enhance CAR-T cell function and promote more effective clearance of heterogenous solid tumors, a strategy that may be further augmented by multi-antigen targeting.

Acknowledgements

We thank Professors Klaus Pfizenmaier (Institute of Cell Biology and Immunology, University of Stuttgart, Stuttgart, Germany), and Stephen Gottschalk (Department of Bone Marrow Transplantation and Cellular Therapy, St Jude Children's Research Hospital, Memphis, TN, USA), for provision of the FAP-specific MO36 scFv. We thank Professor Stuart Pitson, Centre for Cancer Biology, Adelaide, for the kind gift of U251-GFP and U87-RFP. We thank Dr Susanne Heinzel, Walter and Eliza Hall Institute of Medical Research, Melbourne Victoria, Australia, for her review and valuable comments on the manuscript.

References:

1. Field KM, Simes J, Nowak AK, Cher L, Wheeler H, Hovey EJ*, et al.* Randomized phase 2 study of carboplatin and bevacizumab in recurrent glioblastoma. Neuro Oncol **2015**;17(11):1504-13 doi 10.1093/neuonc/nov104.
2. Wagner J, Wickman E, DeRenzo C, Gottschalk S. CAR T Cell Therapy for Solid Tumors: Bright Future or Dark Reality? Mol Ther **2020**;28(11):2320-39 doi 10.1016/j.ymthe.2020.09.015.
3. Brown MP, Ebert LM, Gargett T. Clinical chimeric antigen receptor-T cell therapy: a new and promising treatment modality for glioblastoma. Clin Transl Immunology **2019**;8(5):e1050 doi 10.1002/cti2.1050.
4. Ahmed N, Salsman VS, Kew Y, Shaffer D, Powell S, Zhang YJ*, et al.* HER2-specific T cells target primary glioblastoma stem cells and induce regression of autologous experimental tumors. Clin Cancer Res **2010**;16(2):474-85 doi 10.1158/1078-0432.CCR-09-1322.
5. Brown CE, Badie B, Barish ME, Weng L, Ostberg JR, Chang WC*, et al.* Bioactivity and Safety of IL13Ralpha2-Redirected Chimeric Antigen Receptor CD8+ T Cells in Patients with Recurrent Glioblastoma. Clin Cancer Res **2015**;21(18):4062-72 doi 10.1158/1078-0432.CCR-15-0428.
6. Brown CE, Alizadeh D, Starr R, Weng L, Wagner JR, Naranjo A*, et al.* Regression of Glioblastoma after Chimeric Antigen Receptor T-Cell Therapy. N Engl J Med **2016**;375(26):2561-9 doi 10.1056/NEJMoa1610497.
7. O'Rourke DM, Nasrallah MP, Desai A, Melenhorst JJ, Mansfield K, Morrissette JJD*, et al.* A single dose of peripherally infused EGFRvIII-directed CAR T cells mediates antigen loss and induces adaptive resistance in patients with recurrent glioblastoma. Sci Transl Med **2017**;9(399) doi 10.1126/scitranslmed.aaa0984.
8. Brown CE, Aguilar B, Starr R, Yang X, Chang WC, Weng L*, et al.* Optimization of IL13Ralpha2-Targeted Chimeric Antigen Receptor T Cells for Improved Anti-tumor Efficacy against Glioblastoma. Mol Ther **2018**;26(1):31-44 doi 10.1016/j.ymthe.2017.10.002.
9. Goff SL, Morgan RA, Yang JC, Sherry RM, Robbins PF, Restifo NP*, et al.* Pilot Trial of Adoptive Transfer of Chimeric Antigen Receptor-transduced T Cells Targeting EGFRvIII in Patients With Glioblastoma. J Immunother **2019**;42(4):126-35 doi 10.1097/CJI.0000000000000260.
10. Rettig WJ, Garin-Chesa P, Beresford HR, Oettgen HF, Melamed MR, Old LJ. Cell-surface glycoproteins of human sarcomas: differential expression in normal and malignant tissues and cultured cells. Proc Natl Acad Sci U S A **1988**;85(9):3110-4 doi 10.1073/pnas.85.9.3110.
11. Ostermann E, Garin-Chesa P, Heider KH, Kalat M, Lamche H, Puri C*, et al.* Effective immunoconjugate therapy in cancer models targeting a serine protease of tumor fibroblasts. Clin Cancer Res **2008**;14(14):4584-92 doi 10.1158/1078-0432.CCR-07-5211.
12. Kakarla S, Chow KK, Mata M, Shaffer DR, Song XT, Wu MF*, et al.* Antitumor effects of chimeric receptor engineered human T cells directed to tumor stroma. Mol Ther **2013**;21(8):1611-20 doi 10.1038/mt.2013.110.
13. Wang LC, Lo A, Scholler J, Sun J, Majumdar RS, Kapoor V*, et al.* Targeting fibroblast activation protein in tumor stroma with chimeric antigen receptor T cells can inhibit tumor growth and augment host immunity without severe toxicity. Cancer Immunol Res **2014**;2(2):154-66 doi 10.1158/2326-6066.CIR-13-0027.
14. Lo A, Wang LS, Scholler J, Monslow J, Avery D, Newick K*, et al.* Tumor-Promoting Desmoplasia Is Disrupted by Depleting FAP-Expressing Stromal Cells. Cancer Res **2015**;75(14):2800-10 doi 10.1158/0008-5472.CAN-14-3041.
15. Petrausch U, Schuberth PC, Hagedorn C, Soltermann A, Tomaszek S, Stahel R*, et al.* Re-directed T cells for the treatment of fibroblast activation protein (FAP)-positive malignant pleural mesothelioma (FAPME-1). BMC Cancer **2012**;12:615 doi 10.1186/1471-2407-12-615.

16. Schuberth PC, Hagedorn C, Jensen SM, Gulati P, van den Broek M, Mischo A*, et al.* Treatment of malignant pleural mesothelioma by fibroblast activation protein-specific re-directed T cells. J Transl Med **2013**;11:187 doi 10.1186/1479-5876-11-187.
17. Ebert LM, Yu W, Gargett T, Toubia J, Kollis PM, Tea MN*, et al.* Endothelial, pericyte and tumor cell expression in glioblastoma identifies fibroblast activation protein (FAP) as an excellent target for immunotherapy. Clin Transl Immunology **2020**;9(10):e1191 doi 10.1002/cti2.1191.
18. Li M, Li G, Kiyokawa J, Tirmizi Z, Richardson LG, Ning J*, et al.* Characterization and oncolytic virus targeting of FAP-expressing tumor-associated pericytes in glioblastoma. Acta Neuropathol Commun **2020**;8(1):221 doi 10.1186/s40478-020-01096-0.
19. Tran E, Chinnasamy D, Yu Z, Morgan RA, Lee CC, Restifo NP*, et al.* Immune targeting of fibroblast activation protein triggers recognition of multipotent bone marrow stromal cells and cachexia. J Exp Med **2013**;210(6):1125-35 doi 10.1084/jem.20130110.
20. Gulati P, Ruhl J, Kannan A, Pircher M, Schuberth P, Nytko KJ*, et al.* Aberrant Lck Signal via CD28 Costimulation Augments Antigen-Specific Functionality and Tumor Control by Redirected T Cells with PD-1 Blockade in Humanized Mice. Clin Cancer Res **2018**;24(16):3981-93 doi 10.1158/1078-0432.CCR-17-1788.
21. A. Curioni CB, S. Hiltbrunner, L. Bankel, P. Gulati, W. Weder, I. Opitz,O. Lauk, C. Caviezel, A. Knuth, C.Mu¨nz, C. Renner, R.A. Stahel, U. Petrausch. A phase I clinical trial of malignant pleural mesothelioma treated with locally delivered autologous anti-FAP-targeted CAR T-cells. Annals of Oncology2019.
22. Brocks B, Garin-Chesa P, Behrle E, Park JE, Rettig WJ, Pfizenmaier K*, et al.* Species-crossreactive scFv against the tumor stroma marker "fibroblast activation protein" selected by phage display from an immunized FAP-/- knock-out mouse. Mol Med **2001**;7(7):461-9.
23. Rahman M, Reyner K, Deleyrolle L, Millette S, Azari H, Day BW*, et al.* Neurosphere and adherent culture conditions are equivalent for malignant glioma stem cell lines. Anat Cell Biol **2015**;48(1):25-35 doi 10.5115/acb.2015.48.1.25.
24. Schroeder HW, Jr., Cavacini L. Structure and function of immunoglobulins. J Allergy Clin Immunol **2010**;125(2 Suppl 2):S41-52 doi 10.1016/j.jaci.2009.09.046.
25. Nirula A, Glaser SM, Kalled SL, Taylor FR. What is IgG4? A review of the biology of a unique immunoglobulin subtype. Curr Opin Rheumatol **2011**;23(1):119-24 doi 10.1097/BOR.0b013e3283412fd4.
26. Hudecek M, Sommermeyer D, Kosasih PL, Silva-Benedict A, Liu L, Rader C*, et al.* The nonsignaling extracellular spacer domain of chimeric antigen receptors is decisive for in vivo antitumor activity. Cancer Immunol Res **2015**;3(2):125-35 doi 10.1158/2326-6066.CIR-14-0127.
27. Jonnalagadda M, Mardiros A, Urak R, Wang X, Hoffman LJ, Bernanke A*, et al.* Chimeric antigen receptors with mutated IgG4 Fc spacer avoid fc receptor binding and improve T cell persistence and antitumor efficacy. Mol Ther **2015**;23(4):757-68 doi 10.1038/mt.2014.208 S1525-0016(16)30095-8 [pii].
28. Upadhyay R, Boiarsky JA, Pantsulaia G, Svensson-Arvelund J, Lin MJ, Wroblewska A*, et al.* A Critical Role for Fas-Mediated Off-Target Tumor Killing in T-cell Immunotherapy. Cancer Discov **2021**;11(3):599-613 doi 10.1158/2159-8290.CD-20-0756.
29. Bonnotte B, Favre N, Reveneau S, Micheau O, Droin N, Garrido C*, et al.* Cancer cell sensitization to fas-mediated apoptosis by sodium butyrate. Cell Death Differ **1998**;5(6):480-7 doi 10.1038/sj.cdd.4400371.
30. Monjazeb AM, Hsiao HH, Sckisel GD, Murphy WJ. The role of antigen-specific and non-specific immunotherapy in the treatment of cancer. J Immunotoxicol **2012**;9(3):248-58 doi 10.3109/1547691X.2012.685527.
31. Ma HL, Whitters MJ, Konz RF, Senices M, Young DA, Grusby MJ*, et al.* IL-21 activates both innate and adaptive immunity to generate potent antitumor responses that require perforin

but are independent of IFN-gamma. J Immunol **2003**;171(2):608-15 doi 10.4049/jimmunol.171.2.608.

32. Smyth MJ, Swann J, Kelly JM, Cretney E, Yokoyama WM, Diefenbach A*, et al.* NKG2D recognition and perforin effector function mediate effective cytokine immunotherapy of cancer. J Exp Med **2004**;200(10):1325-35 doi 10.1084/jem.20041522.

33. Liu RB, Engels B, Schreiber K, Ciszewski C, Schietinger A, Schreiber H*, et al.* IL-15 in tumor microenvironment causes rejection of large established tumors by T cells in a noncognate T cell receptor-dependent manner. Proc Natl Acad Sci U S A **2013**;110(20):8158-63 doi 10.1073/pnas.1301022110.

34. Wensveen FM, Jelencic V, Polic B. NKG2D: A Master Regulator of Immune Cell Responsiveness. Front Immunol **2018**;9:441 doi 10.3389/fimmu.2018.00441.

35. Busek P, Balaziova E, Matrasova I, Hilser M, Tomas R, Syrucek M*, et al.* Fibroblast activation protein alpha is expressed by transformed and stromal cells and is associated with mesenchymal features in glioblastoma. Tumour Biol **2016**;37(10):13961-71 doi 10.1007/s13277-016-5274-9.

36. Perrin SL, Samuel MS, Koszyca B, Brown MP, Ebert LM, Oksdath M*, et al.* Glioblastoma heterogeneity and the tumour microenvironment: implications for preclinical research and development of new treatments. Biochem Soc Trans **2019**;47(2):625-38 doi 10.1042/BST20180444.

37. Allegra A, Alonci A, Penna G, Innao V, Gerace D, Rotondo F*, et al.* The cancer stem cell hypothesis: a guide to potential molecular targets. Cancer Invest **2014**;32(9):470-95 doi 10.3109/07357907.2014.958231.

38. Pollard SM, Yoshikawa K, Clarke ID, Danovi D, Stricker S, Russell R*, et al.* Glioma stem cell lines expanded in adherent culture have tumor-specific phenotypes and are suitable for chemical and genetic screens. Cell Stem Cell **2009**;4(6):568-80 doi 10.1016/j.stem.2009.03.014.

39. Galli R, Binda E, Orfanelli U, Cipelletti B, Gritti A, De Vitis S*, et al.* Isolation and characterization of tumorigenic, stem-like neural precursors from human glioblastoma. Cancer Res **2004**;64(19):7011-21 doi 10.1158/0008-5472.CAN-04-1364.

40. Stringer BW, Day BW, D'Souza RCJ, Jamieson PR, Ensbey KS, Bruce ZC*, et al.* A reference collection of patient-derived cell line and xenograft models of proneural, classical and mesenchymal glioblastoma. Sci Rep **2019**;9(1):4902 doi 10.1038/s41598-019-41277-z.

41. Fleischer B. Lysis of bystander target cells after triggering of human cytotoxic T lymphocytes. Eur J Immunol **1986**;16(8):1021-4 doi 10.1002/eji.1830160826.

42. Lanzavecchia A. Is the T-cell receptor involved in T-cell killing? Nature **1986**;319(6056):778-80 doi 10.1038/319778a0.

43. Hong LK, Chen Y, Smith CC, Montgomery SA, Vincent BG, Dotti G*, et al.* CD30-Redirected Chimeric Antigen Receptor T Cells Target CD30(+) and CD30(-) Embryonal Carcinoma via Antigen-Dependent and Fas/FasL Interactions. Cancer Immunol Res **2018**;6(10):1274-87 doi 10.1158/2326-6066.CIR-18-0065.

44. Benmebarek MR, Karches CH, Cadilha BL, Lesch S, Endres S, Kobold S. Killing Mechanisms of Chimeric Antigen Receptor (CAR) T Cells. Int J Mol Sci **2019**;20(6) doi 10.3390/ijms20061283.

45. Zaidi MR. The Interferon-Gamma Paradox in Cancer. J Interferon Cytokine Res **2019**;39(1):30-8 doi 10.1089/jir.2018.0087.

46. Idriss HT, Naismith JH. TNF alpha and the TNF receptor superfamily: structure-function relationship(s). Microsc Res Tech **2000**;50(3):184-95 doi 10.1002/1097-0029(20000801)50:3<184::AID-JEMT2>3.0.CO;2-H.

47. Michie J, Beavis PA, Freeman AJ, Vervoort SJ, Ramsbottom KM, Narasimhan V*, et al.* Antagonism of IAPs Enhances CAR T-cell Efficacy. Cancer Immunol Res **2019**;7(2):183-92 doi 10.1158/2326-6066.CIR-18-0428.

48. Gehrmann M, Stangl S, Kirschner A, Foulds GA, Sievert W, Doss BT*, et al.* Immunotherapeutic targeting of membrane Hsp70-expressing tumors using recombinant human granzyme B. PLoS One **2012**;7(7):e41341 doi 10.1371/journal.pone.0041341.
49. Trapani JA. Granzymes: a family of lymphocyte granule serine proteases. Genome Biol **2001**;2(12):REVIEWS3014 doi 10.1186/gb-2001-2-12-reviews3014.
50. Murphy WJ, Welniak L, Back T, Hixon J, Subleski J, Seki N*, et al.* Synergistic anti-tumor responses after administration of agonistic antibodies to CD40 and IL-2: coordination of dendritic and CD8+ cell responses. J Immunol **2003**;170(5):2727-33 doi 10.4049/jimmunol.170.5.2727.
51. Berner V, Liu H, Zhou Q, Alderson KL, Sun K, Weiss JM*, et al.* IFN-gamma mediates CD4+ T-cell loss and impairs secondary antitumor responses after successful initial immunotherapy. Nat Med **2007**;13(3):354-60 doi 10.1038/nm1554.
52. Sparrow E, Bodman-Smith MD. Granulysin: The attractive side of a natural born killer. Immunol Lett **2020**;217:126-32 doi 10.1016/j.imlet.2019.11.005.
53. Wu CH, Li J, Li L, Sun J, Fabbri M, Wayne AS*, et al.* Extracellular vesicles derived from natural killer cells use multiple cytotoxic proteins and killing mechanisms to target cancer cells. J Extracell Vesicles **2019**;8(1):1588538 doi 10.1080/20013078.2019.1588538.
54. Muroya M, Chang K, Uchida K, Bougaki M, Yamada Y. Analysis of cytotoxicity induced by proinflammatory cytokines in the human alveolar epithelial cell line A549. Biosci Trends **2012**;6(2):70-80.
55. Kim TS, Shin EC. The activation of bystander CD8(+) T cells and their roles in viral infection. Exp Mol Med **2019**;51(12):1-9 doi 10.1038/s12276-019-0316-1.
56. Rosenberg SA. IL-2: the first effective immunotherapy for human cancer. J Immunol **2014**;192(12):5451-8 doi 10.4049/jimmunol.1490019.
57. Rollings CM, Sinclair LV, Brady HJM, Cantrell DA, Ross SH. Interleukin-2 shapes the cytotoxic T cell proteome and immune environment-sensing programs. Sci Signal **2018**;11(526) doi 10.1126/scisignal.aap8112.
58. Maykel J, Liu JH, Li H, Shultz LD, Greiner DL, Houghton J. NOD-scidIl2rg (tm1Wjl) and NOD-Rag1 (null) Il2rg (tm1Wjl) : a model for stromal cell-tumor cell interaction for human colon cancer. Dig Dis Sci **2014**;59(6):1169-79 doi 10.1007/s10620-014-3168-5.
59. Zhou Y, Husman T, Cen X, Tsao T, Brown J, Bajpai A*, et al.* Interleukin 15 in Cell-Based Cancer Immunotherapy. Int J Mol Sci **2022**;23(13) doi 10.3390/ijms23137311.
60. Gargett T, Ebert LM, Truong NTH, Kollis PM, Sedivakova K, Yu W*, et al.* GD2-targeting CAR-T cells enhanced by transgenic IL-15 expression are an effective and clinically feasible therapy for glioblastoma. J Immunother Cancer **2022**;10(9) doi 10.1136/jitc-2022-005187.
61. Allen GM, Frankel NW, Reddy NR, Bhargava HK, Yoshida MA, Stark SR*, et al.* Synthetic cytokine circuits that drive T cells into immune-excluded tumors. Science **2022**;378(6625):eaba1624 doi 10.1126/science.aba1624.
62. Oyler-Yaniv A, Oyler-Yaniv J, Whitlock BM, Liu Z, Germain RN, Huse M*, et al.* A Tunable Diffusion-Consumption Mechanism of Cytokine Propagation Enables Plasticity in Cell-to-Cell Communication in the Immune System. Immunity **2017**;46(4):609-20 doi 10.1016/j.immuni.2017.03.011.

Figure 1

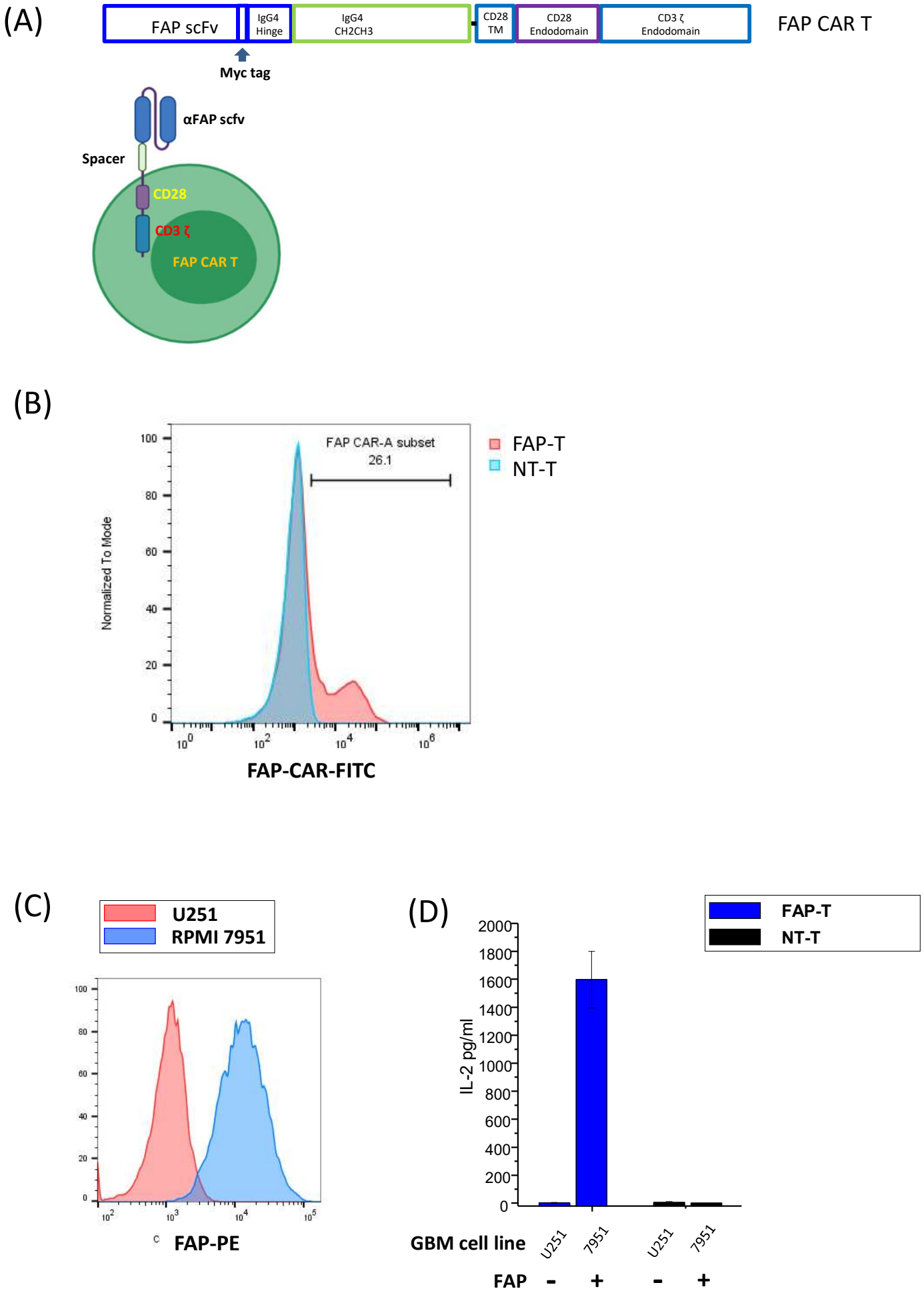

Figure 1. **Structure and expression of FAP CARs. (A)** Schematic representation of the FAP CAR construct. The CAR consisted of anti-FAP scFv linked to a CD28 costimulatory domain and CD3ζ. FAP CAR contains the myc tag at the end of the scFv and a spacer from human IgG4 CH2CH3 fragment with modifications. **(B)** CAR expression on CAR-T cells was detected by flow cytometry. The CAR-T cells were stained by FITC conjugated anti-myc tag antibody. **(C)** FAP expression on target cell lines was confirmed by flow cytometry. **(D)** CAR-transduced or non-transduced T cells were co-cultured with target cells and the IL-2 concentration in supernatants determined 48 hours later. Data represent mean +/- SD from triplicate wells.

Figure 2

(A) GBM long term cell lines

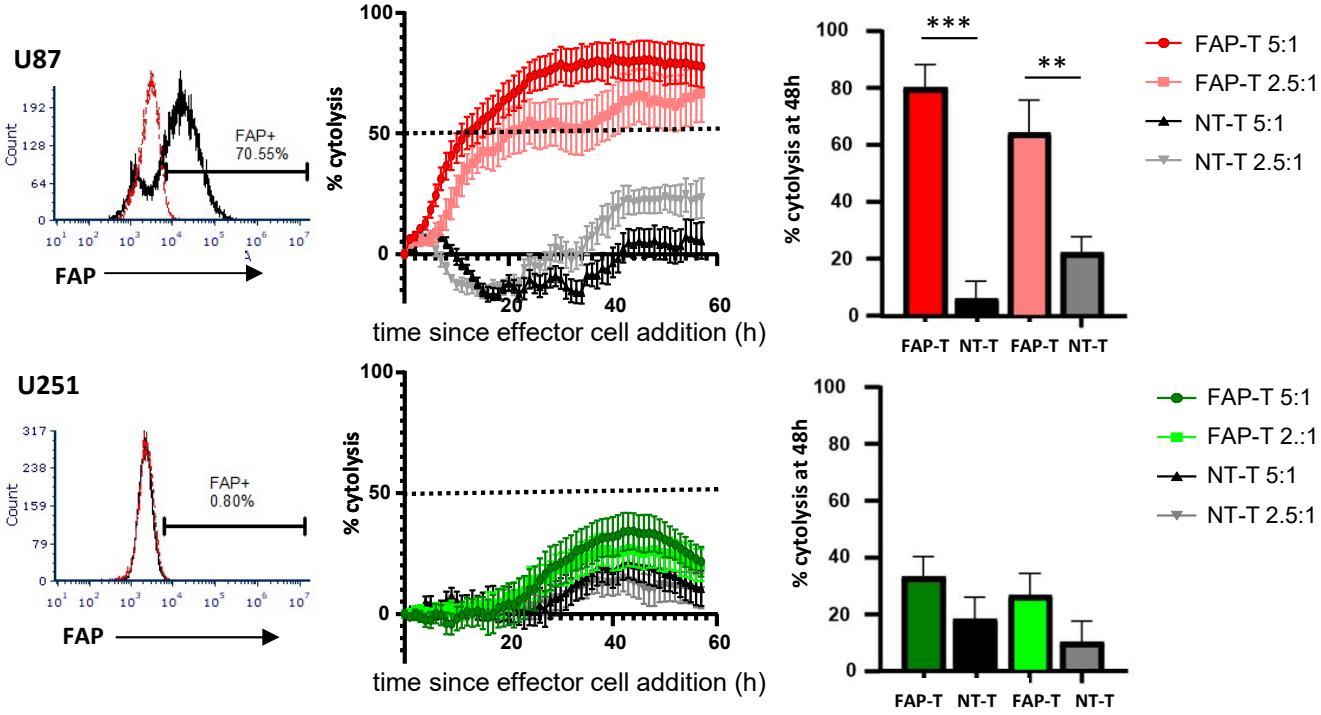

(B) GNS cells

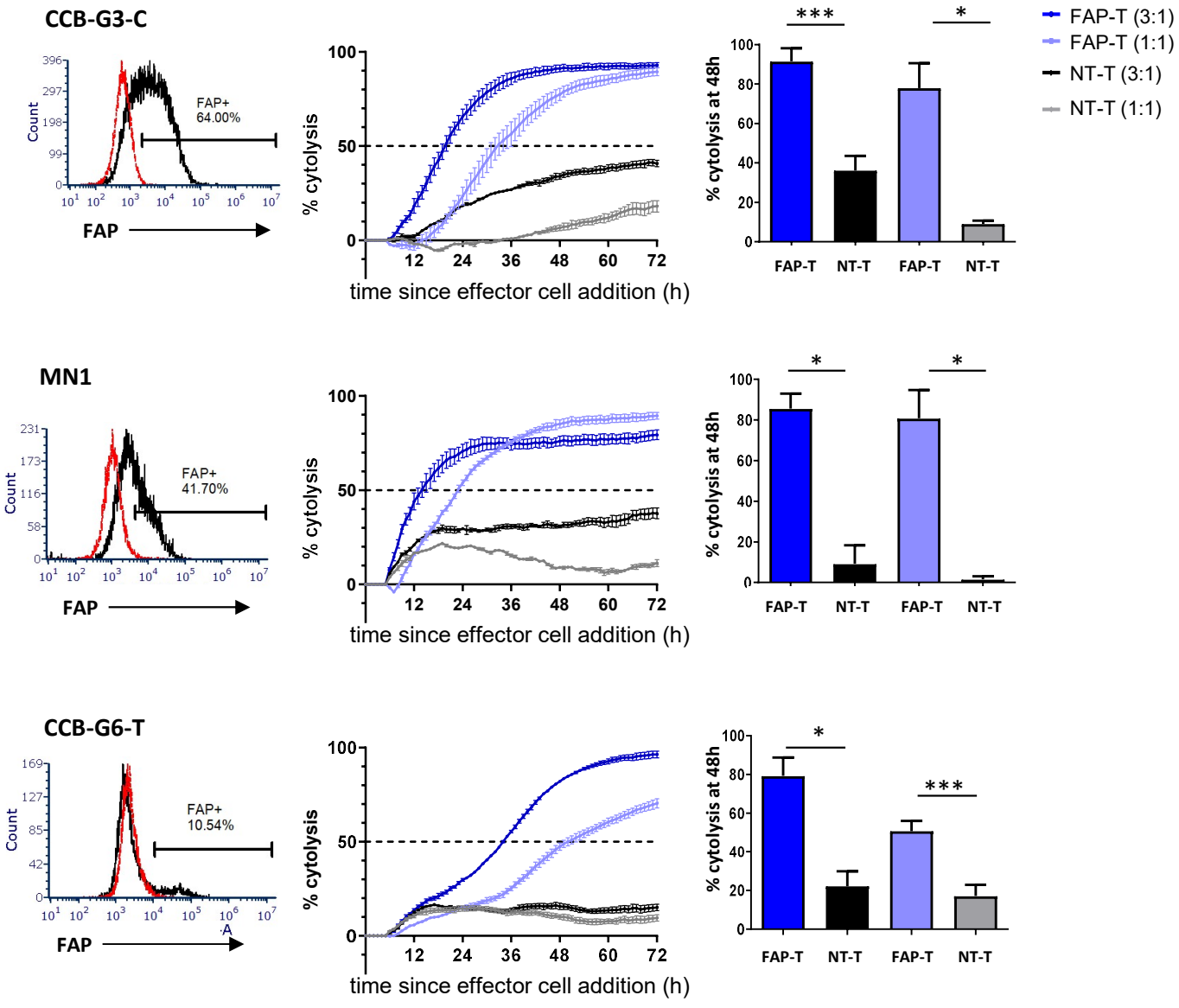

Figure 2. FAP-T display cytotoxic activity against glioblastoma cell lines and GNS cells expressing varying levels of FAP. Left panels: FAP expression on target cells was examined by flow cytometry; red dotted lines indicate isotype control while black solid lines indicate anti-FAP antibody. Centre and right panels: Target cells were established in a CytoView-Z plate and placed in the Maestro Z system for up to 24 hours, followed by addition of FAP-T as effectors or non transduced T cells (NT-T) as control. Cytotoxicity was monitored over time and represented as percentage of target lysis averaged across duplicate wells. Representative examples shown in centre panels and % cytolysis at 48 hours after effector cell addition is plotted on the right panels (mean and SEM from 3-4 experiments). The effector:target (E:T) ratio is indicated. **(A)** FAP(+) U87 and FAP(-) U251 cells were used as target cells. **(B)** GNS cells expressing varying levels of FAP were used as target cells.

Figure 3

(A)

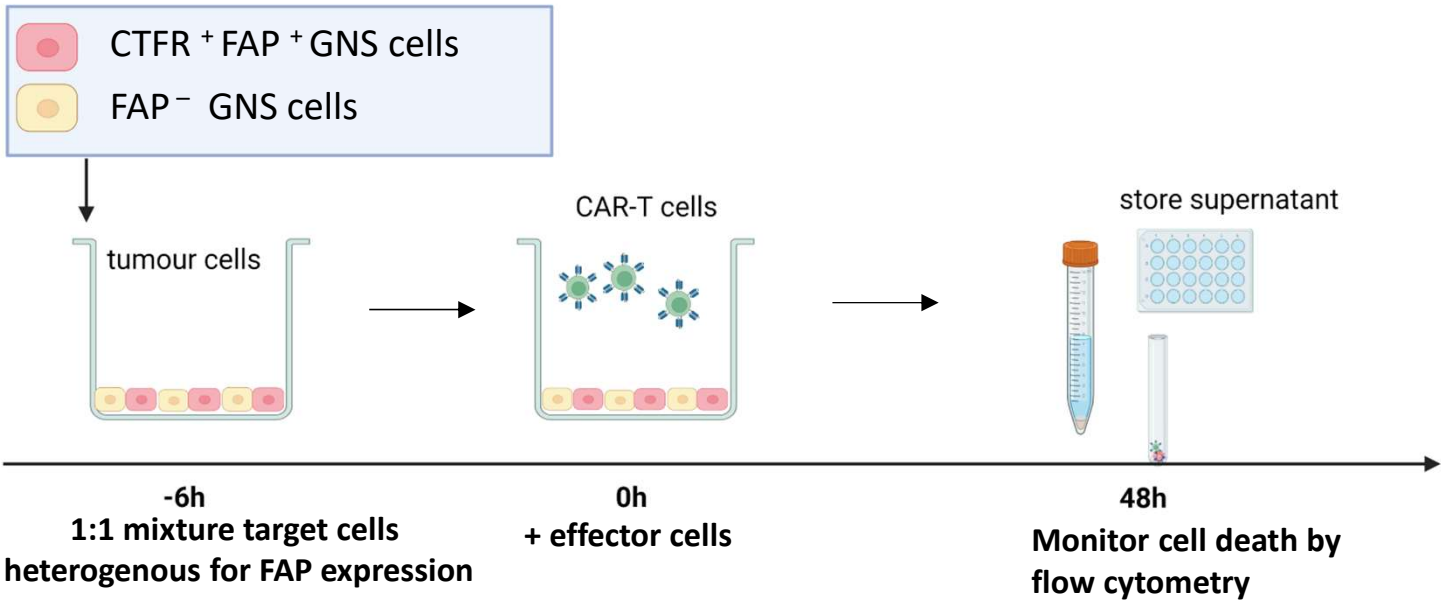

(B)

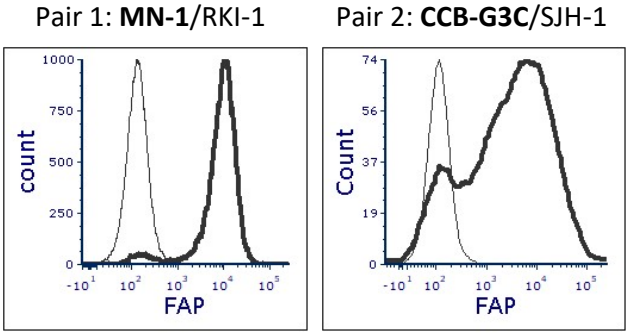

(D)

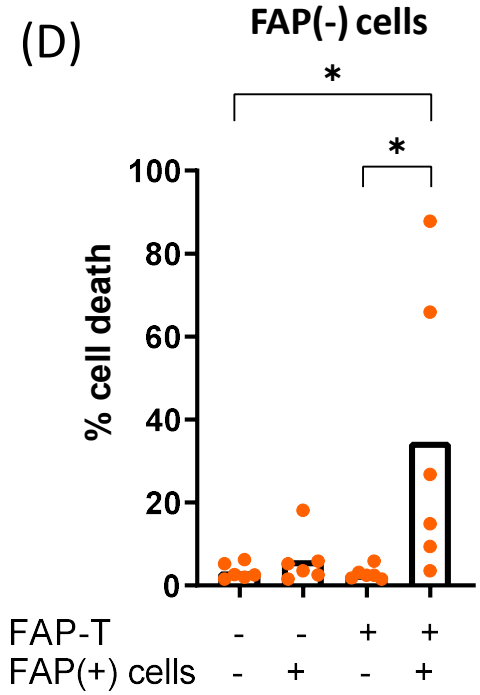

(C)

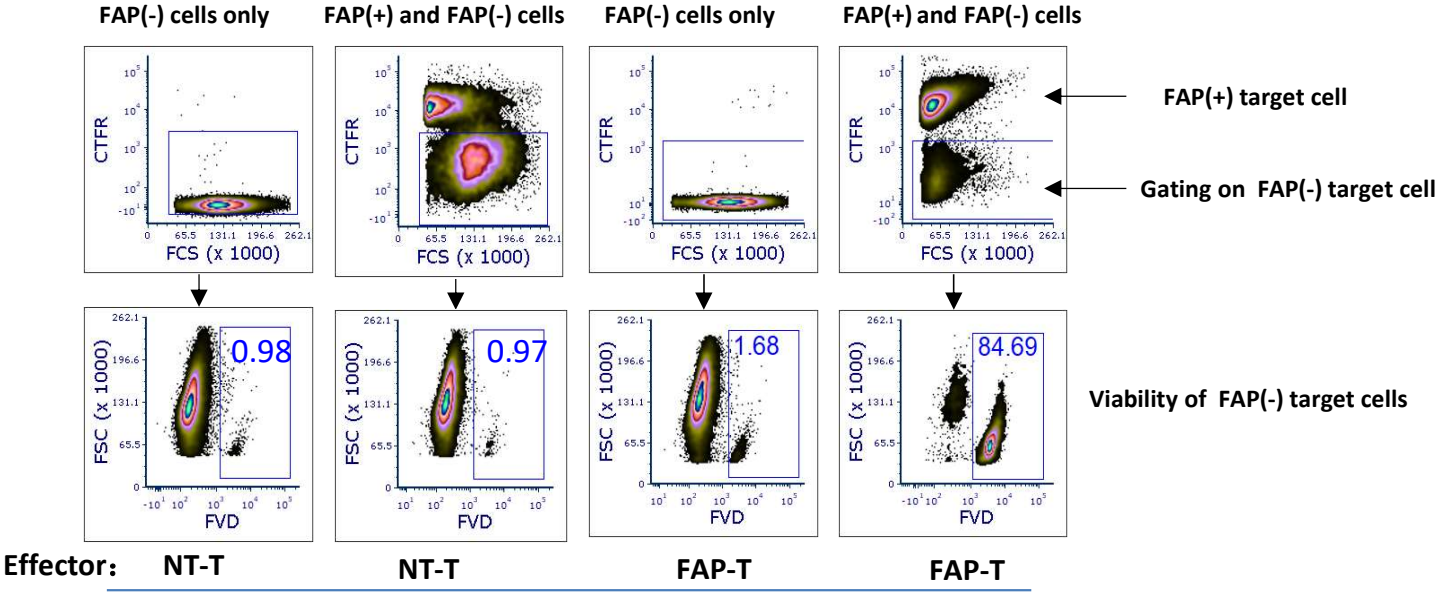

Figure 3: FAP-T cells exert a bystander killing effect on FAP(-) tumor cells after CAR engagement. **(A)** Schema illustrates the workflow of co-culture assay: FAP(+) and FAP(-) tumor cells were mixed at 1:1 ratio and treated with either FAP-T cells or non transduced T cells (NT-T) at 1:1 E:T ratio. Single cultured target cells were treated in the same way as control (not illustrated). The viability of target cells was analyzed 48 hours later by flow cytometry. **(B)** Surface expression of FAP on two pairs of target cell lines: FAP(+) MN-1 and FAP(-) RKI-1 on the left, and FAP(+) CCB-G3C and FAP(-) SJH-1 on the right. **(C)** Gating strategy of representative examples from left to right: FAP(-) single tumor plus NT-T cells; FAP(+/-) mixed cells plus NT-T cells; FAP(-) single tumor plus FAP-T cells; FAP(+/-) mixed cells plus FAP-T cells. FAP(+) tumor cells were stained with cell trace far red (CTFR) for discrimination. Fixable viability dye (FVD) was used for viability assay. **(D)** The percentage of cell death of FAP(-) GNS after 48h co-culture from all tests was plotted. Data was pooled from three independent experiments. t test; *$p<0.05$, **$p<0.005$ ($n=6$).

Figure 4

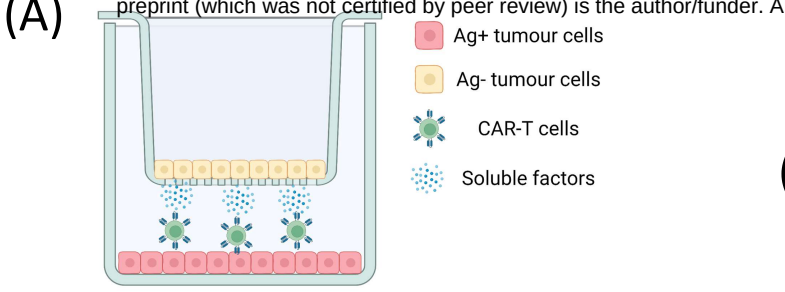

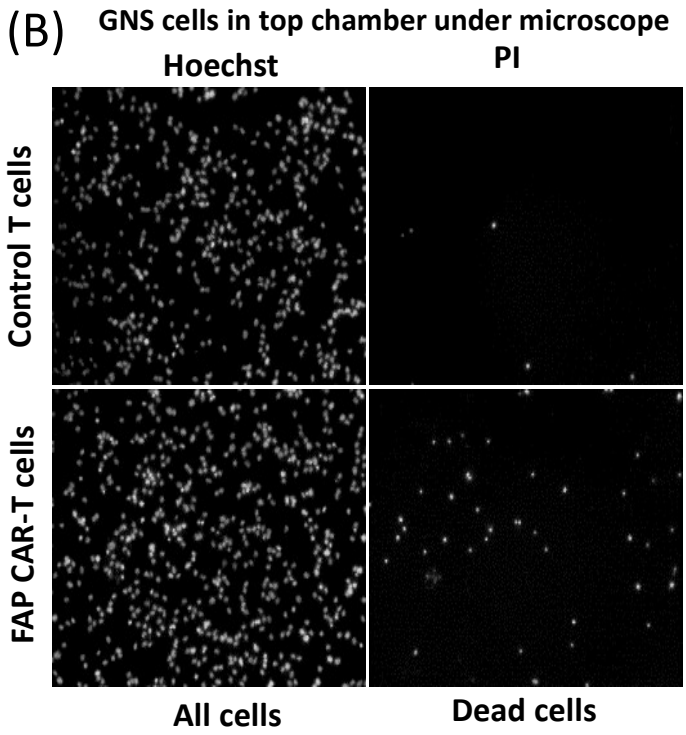

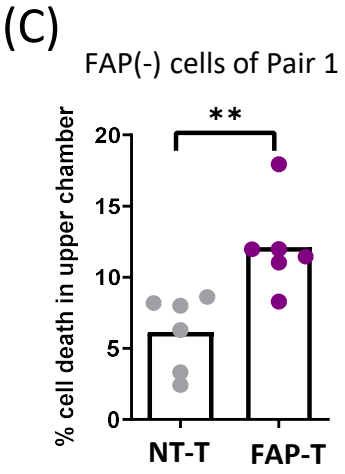

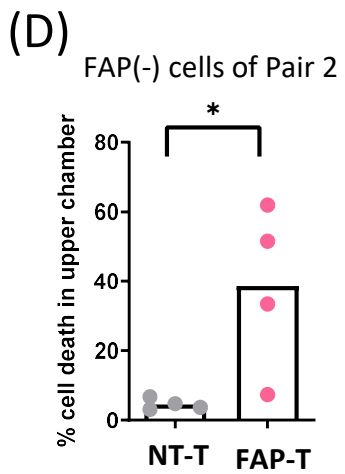

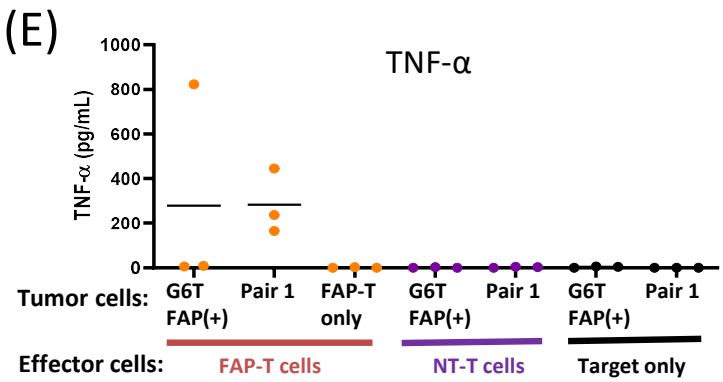

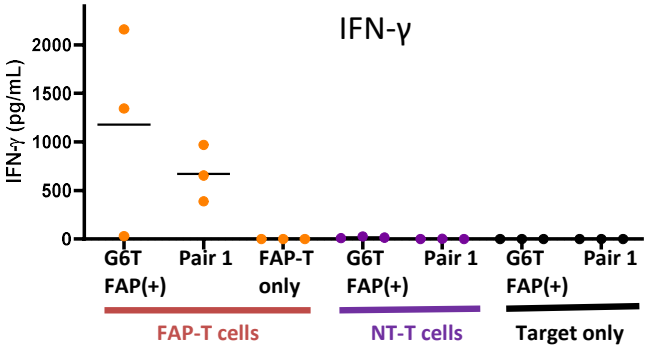

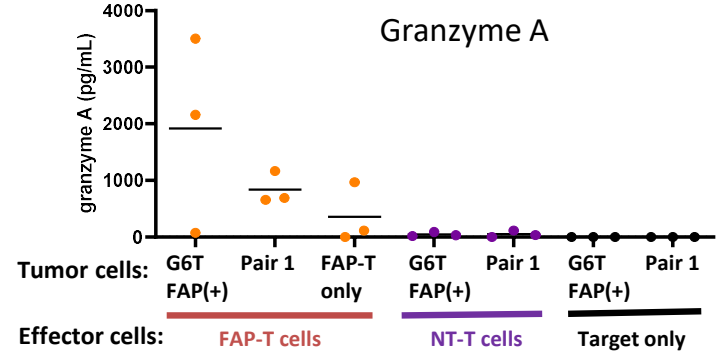

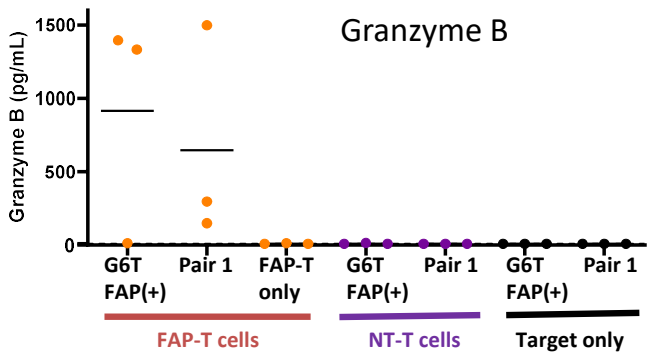

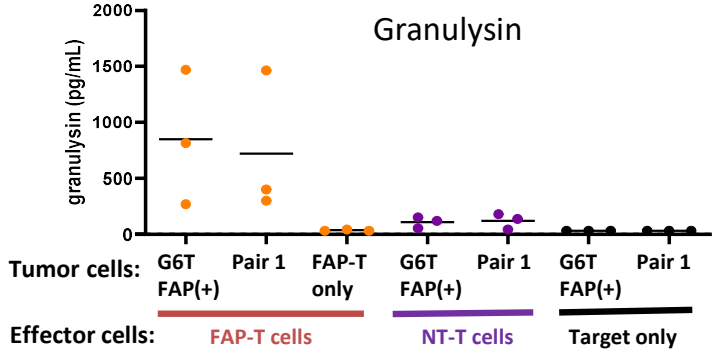

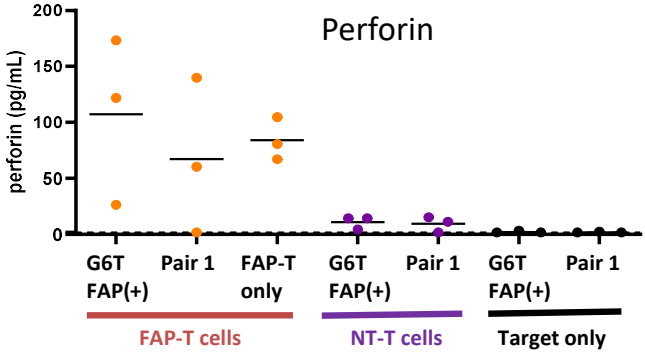

Figure 4: Bystander killing by FAP-T cells can be mediated by soluble factors. (A) Schematic of assay set-up. **(B)** Representative fluorescent images of Hoechst 33258 (left) and PI (right) staining on FAP(-) tumor cells cultured in upper chambers for 48 hours. Effector cells (NT-T cells or FAP-T cells) added to lower chambers are indicated. Images were collected using a 10X objective. **(C-D)** Quantification of percent of FAP(-) target cell death in upper chamber. Shown in **C** is RKI-1 from Pair 1, n = 6, pooled from 3 experiments. Shown in **D** is SJH-1 from Pair 2, n = 4 pooled from 2 experiments. Each dot represents the mean percentage of cell death from 3 fields of view of each well. **(E)** Concentrations of secreted factors in supernatants of Pair 1 cocultures were determined by Legendplex kit. FAP-T stimulated by the FAP(+) GNS cell line CCB-G6T was used as positive control. Supernatants were collected after 48 hours. Data are pooled from 3 experiments.

Figure 5

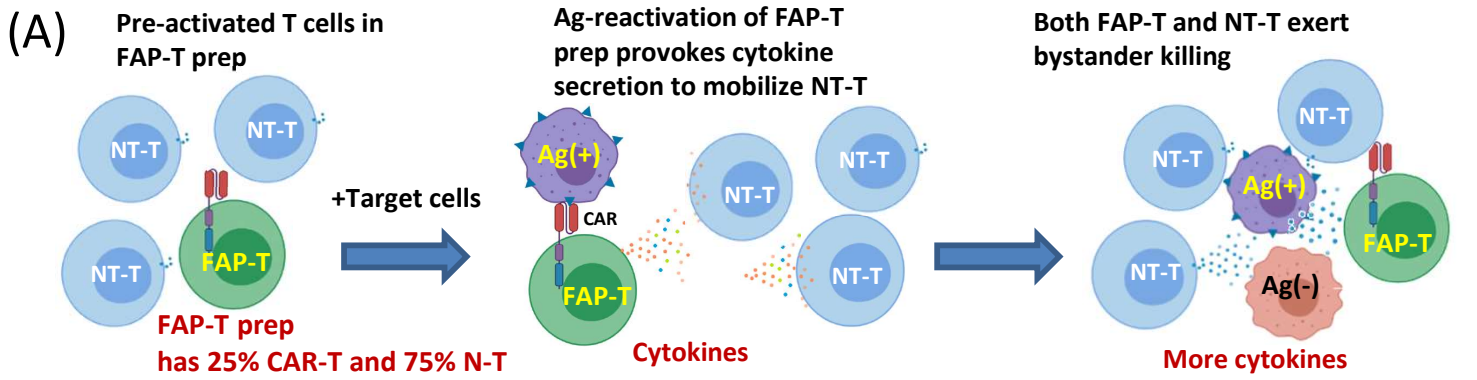

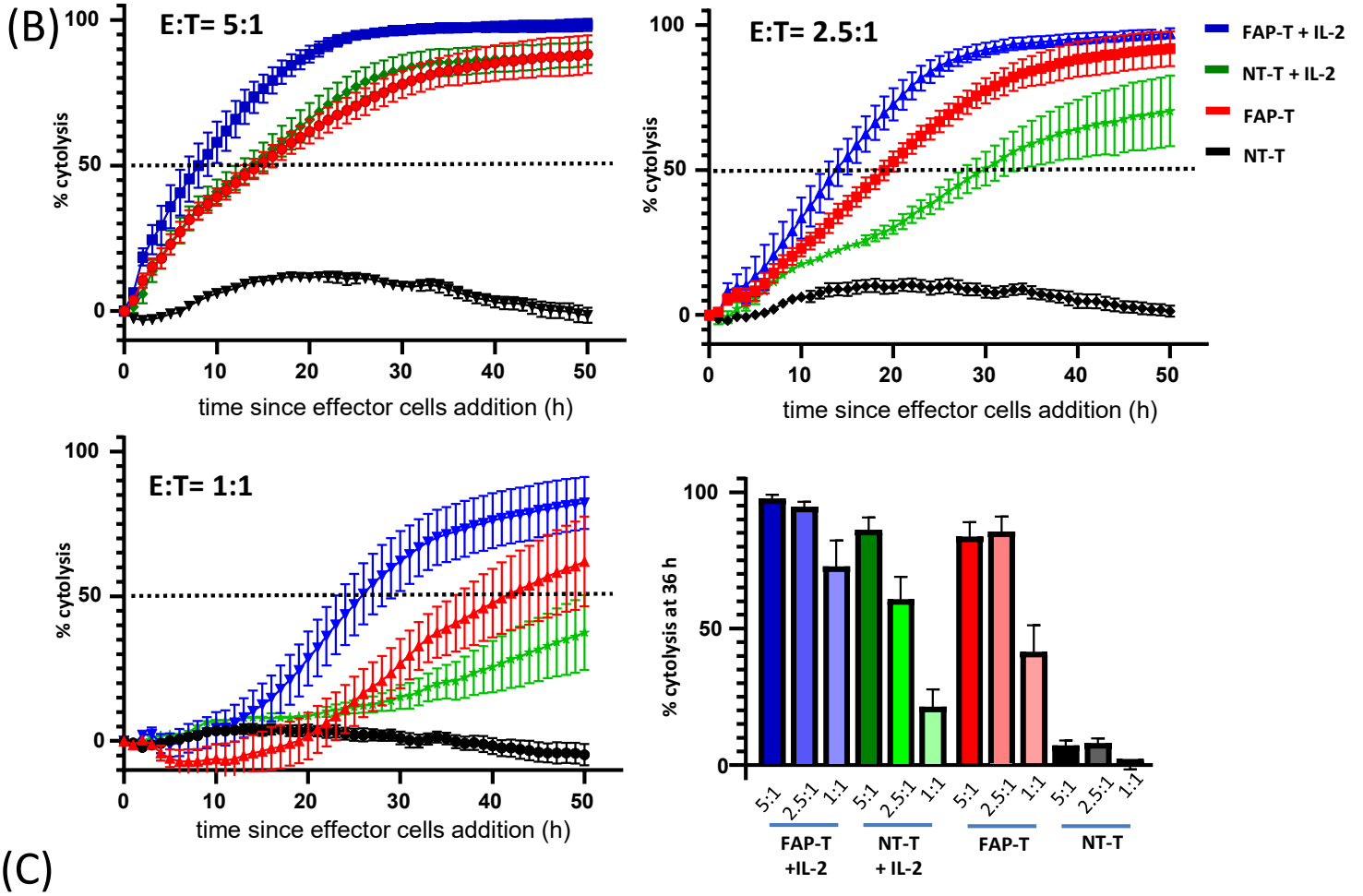

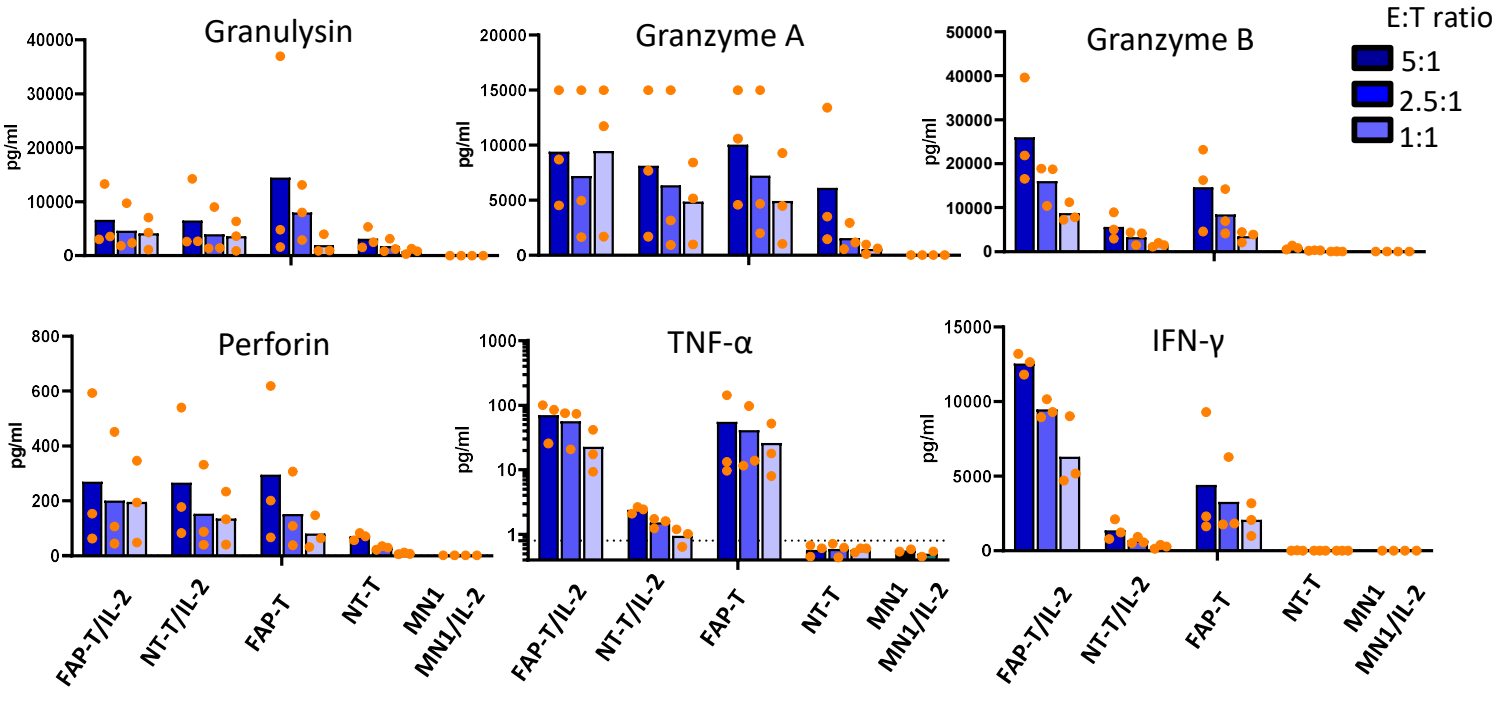

Figure 5. IL-2 induces T cells to exert antigen nonspecific cytotoxicity against GNS cells. (A) A conceptual diagram of the theory. After antigen-specific activation, FAP-T cells secrete IL-2 which mobilizes NT-T cells to exert further cytotoxicity against tumor cells. **(B)** Cytotoxicity assay of FAP-T or NT-T cells against MN1 GNS cells, with or without exogenous IL-2. FAP(+) MN1 cells were established in a CytoView-Z plate for 24 hours prior to addition of effector cells. Target cell growth was monitored by impedance values in real time by the Maestro Z system. Time-course graphs for varying E:T ratios, as indicated, show target lysis as % cytotoxicity. A summary of % cytolysis at 36 hours after effector cell addition is shown bottom right. Data points represent mean +/- SEM for 6 readings from 3 independent experiments. **(C)** Secreted factors were measured in supernatants 50 hours after addition of effector cells using Legendplex assay. A total of 13 analytes were measured in 3 experiments (or 2 experiments for MN-1 and MN-1/IL-2 controls). Results of 6 key cytotoxic factors are shown, with the other 7 being depicted in Figure S4.

Figure 6

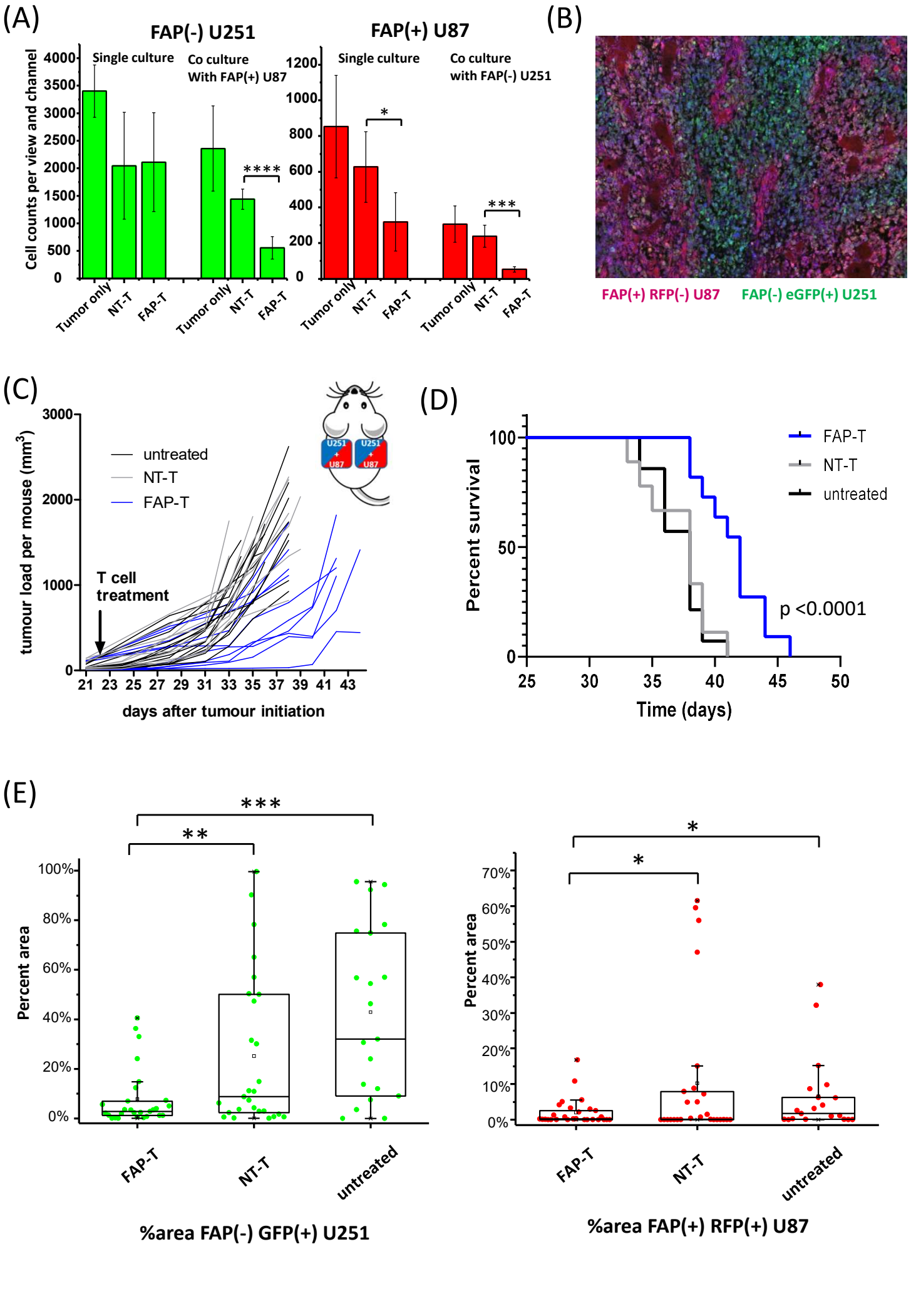

Figure 6. FAP-T cells control tumor growth in a mouse model with heterogeneous antigen expression. (A) In vitro bystander killing assay of FAP(-) U251-GFP and FAP(+) U87-RFP. Cells were cultured individually or together and were treated with FAP-T or NT-T cells. Fluorescent images were taken 24 hours later and GFP and RFP positive cells were counted using ImageJ. Data are from duplicate samples, with 3 fields of view imaged and counted per sample. Graphs show mean and SD from 6 counts. **(B-E)** Subcutaneous tumours were created on both flanks of NSG mice using a mixture of U251-GFP and U87-GFP cells (as illustrated in the inset to C). Tumors were allowed to establish for 21 days and then mice were treated with a single intravenous injection of 1 x 10^6 FAP-T cells (blue) or NT-T cells (grey) or left untreated (black). FAP-T group n=11, NT-T group n=9, untreated group n=14. **(B)** Representative tumor tissue section showing the balance of U251 (green) and U87 (red) cells, with DAPI staining to visualize nuclei. **(C)** Tumor growth curves for each mouse. The volume of tumors on each flank was measured every 2-3 days and summed to calculate total tumor load per mouse. **(D)** Animals were humanely killed once at least one tumor reached 1000 mm^3 and survival analysis performed using a Kaplan–Meier plot. **(E)** GFP and RFP area of endpoint tumour sections were calculated. Data are pooled from a total of 28 sections from 13 tumours of FAP-T treated group, 27 sections from 13 tumors of NT-T treated group and 20 sections from 9 tumors of untreated group.

Table 1

Cytokines	Correlation with cytotoxicity		IL-2/N-T vs N-T (Significant or not)	IL-2/N-T vs IL-2/FAP-T (Significant or not)
	Adj-R2	P value		
Granzyme B	0.47994	8.66E-07	Yes	Yes
IL-4	0.43468	4.06E-06	Yes	Yes
IFN γ	0.43145	4.51E-06	Yes	Yes
Perforin	0.29523	2.52E-04	Yes	**No**
Granzyme A	0.27994	3.78E-04	Yes	Yes
IL-6	0.26234	5.99E-04	Yes	Yes
TNFα	0.25307	7.60E-04	Yes	Yes
IL-10	0.22098	0.00171	**No**	Yes
IL-17a	0.20964	0.00226	**No**	Yes
Granulysin	0.14905	0.00962	Yes	Yes
sFas	-0.02626	**0.81865**	Yes	Yes
sFas L	-0.02713	**0.88065**	Yes	Yes

Table 1. Linear fitting regression was performed using cytolysis%$_{36h}$ vs cytokine concentration$_{(pg/ml)}$. The cytokines were ranked by their adjusted R^2 value from high to low in the table. P value was calculated by ANOVA. The significance of differences between NT-T +/-IL2 or between NT-T and FAP-T was determined by paired t test. $P<0.05$ was considered significant.